

LRP 340/88

January 1988

A NON PERTURBATIVE OPTICAL PROBE FOR LASER
INDUCED FLUORESCENCE DIAGNOSTICS IN
MAGNETIZED PLASMA

F. Anderegg, P.J. Paris, F. Skiff, T.N. Good, M.Q. Tran

A NON PERTURBATIVE OPTICAL PROBE FOR LASER INDUCED FLUORESCENCE DIAGNOSTICS
IN MAGNETIZED PLASMA

F. Anderegg, P.J. Paris, F. Skiff, T.N. Good, M.Q. Tran

Centre de Recherches en Physique des Plasmas
Ecole Polytechnique Fédérale de Lausanne
Association EURATOM - Confédération Suisse
21, Av. des Bains, CH-1007 Lausanne

ABSTRACT

An "optical carriage" has been developed to improve plasma access for LIF diagnostics. Laser light inducing the fluorescence is transported through an optical fiber to the carriage. A telescope fixed on the carriage collects the plasma fluorescence light and sends it through a fiber bundle to an external PMT. The whole carriage is mounted on rails and can be scanned along and across magnetic field. Wave interferograms and slow rotation of a plasma column measured via LIF and optical tagging demonstrate the flexibility of the "optical carriage".

The purpose of this letter is to describe an "optical carriage" which has been designed for the LMP experiment. The first Section gives a brief introduction to laser induced fluorescence (LIF) and to optical tagging. Section II and III describe the LMP device and the optical probe. Typical applications and preliminary results are presented in Section IV.

I INTRODUCTION

The Laser Induced Fluorescence (LIF) technique is based on laser excitation of transitions between quantum states of ions (or neutral atoms) in a plasma.¹ The principle is illustrated in Fig. 1(a). A tunable laser induces transitions (A→B) between two electronic states. Fluorescence light from the spontaneous decay of the state B is collected and analysed. If the laser linewidth is less than the Doppler linewidth, the absorption and fluorescence is due only to those ions for which the laser frequency is at the resonance frequency in the ion rest-frame :

$$\omega_{\text{resonant}} = \omega_{\text{laser}} - k_{\text{laser}} \cdot v_{\text{ion}}$$

This method is able to measure ion densities, velocities (Doppler shift), temperatures (Doppler broadening), electron temperature (density of states), and magnetic fields (Zeeman splitting). Indirectly, even weak electric fields can be measured^{2,7}.

A variant of LIF is optical tagging³. A long lived metastable state, labelled C in Fig. 1(a), is selectively populated by laser excitation of an ionic transition (A → B). This population is created in the volume defined by the intersection of the laser beam with the plasma. The population of A (target state) is correspondingly depleted. The changed populations in this "tagged" volume now propagate into the plasma volume

according to the individual particle trajectories. Having the same mass and charge as ions in the target state (A), the metastable ions may be used as test particles. Information concerning the trajectories of these test particles can be determined by detecting the state population variations which propagate with them. A search laser is used to detect the appearance of test particles, at various positions in the plasma volume.

This technique requires a set of optically interconnected levels of which one is well populated (A1) and the other long lived (metastable); see Fig. 1(b). In addition to positional information, tagging can also determine the velocity-space motion of a particular group of ions with a given initial velocity. The ions must not only pass through both of the spatially separated beams, but they must also have the resonant velocity at each beam.

A tagging experiment can be performed in one of two ways : A) bright signal and B) dark signal.

- A) For bright signal tagging, the search beam detects, the increase in the population of state C by means of a second transition (C - B₂). Observation of fluorescence at λ_4 is a measure of this population.
- B) Dark signal tagging involves measuring the depletion of the target state A (which corresponds to the presence of state C). In this case the search beam may come from the same laser as was used to tag. The reduction in fluorescence from the transition A - B indicates the presence of test particles.

II LMP DEVICE

The linear magnetized plasma device (LMP) ⁴ consists of a grounded stainless steel vacuum vessel (diameter 40cm, length 9.18m) with a magnetic field up to 3kG homogeneous over 20cm diameter and 4.75m length to better than $\Delta B/B=0.3\%$. To compensate thermal drift, the current in the magnetic field coil is controlled by a micro-processor. The LMP device can produce two kinds of plasma : noble gas discharge and alkaline Q-plasma ⁵. In both cases the plasma diameter is 5cm and length up to 4.75m.

III OPTICAL PROBE

Plasma access is generally a delicate problem, especially in the case of magnetized plasma. An optical carriage has been designed to facilitate the transport of light both to and from the plasma. We have chosen to transport the laser light, which is used to induce fluorescence, with an optical fiber and to transport the fluorescent light with another fiber. The use of fibers allows a greater flexibility in carriage position while maintaining optical alignment.

A schematic view of the "optical carriage" in the vacuum vessel is shown in Fig. 2. The laser beam and the telescope line of sight are orthogonal in order to reduce the effect of directly scattered light. In addition, this geometry optimizes spatial resolution by minimizing the diagnosed volume given by the intersection of the viewing volume and the laser path in the plasma.

Laser light is injected into the input fiber with a simple lens mounted on a stable assembly. The required focal length depends on the laser beam divergence and fiber size; the focal length F.L. varies from 10cm to 2mm. Small focal lengths are

achieved by means of a microscope objective. A large diameter quartz fiber (Huber Suhner FO 27120) with $\phi_{\text{core}}=200\mu\text{m}$, $\phi_{\text{cladding}}=280\mu\text{m}$ has been chosen to withstand the high power of a pulsed laser. The fiber is protected with a FEP coating and the portion which is not under vacuum has an extra mechanical protection made of a plastic tube reinforced with Kevlar fiber. A connector (Huber Suhner 9840.14.B) is mounted on the fiber before the vacuum feedthrough to facilitate alignment of the injected light. Because a connector which can support vacuum was not available, the vacuum interface was made by passing bare fiber through a plug of "Torr seal" (made by Varian).

Light at the output of the fiber is collimated by a lens (F.L.=10.5cm) and polarised by a dichroic filter. Polarized light is necessary to select different Zeeman components. The laser beam crosses the plasma and is absorbed in a beam dump mounted on the carriage. The observation telescope is a combined reflector-refractor which achieves a lower f-number than a pure refractor. A suitable mirror (F.L. \cong 51mm) is obtained by covering the concave surface of a F.L.=200mm plano-concave lens of 50mm diameter with enhanced aluminum coating. Aspheric antireflection coated, and plano-convex lenses are used to focalise the light onto a large bundle of glass fiber ($\phi=3.2\text{mm}$). The complete detection telescope has a $f/1.41$. The fiber bundle sends the light to a lens (F.L.=20mm) which is used as a vacuum feedthrough. A series of lenses image the output of the fiber on a PMT. An interference filter with a bandwidth between 1-10nm is used to discriminate against background light. Ion velocity selection using the Doppler effect is made by tuning the laser wavelength λ_1 .

The sigma shape of the optical carriage frame (called below the "sigma") has been chosen to avoid collisions, with probes in the vacuum vessel and to maintain plasma access for probes and antennae while the carriage is moving. A simple

reflective probe can be inserted through a hole of the "sigma" in order to adjust the alignment of the outside elements and, for the use of a pulsed laser, the timing of gated amplifiers used in the fluorescence detection circuit.

Three stainless steel rods guide the carriage over a distance of 182cm along the axis of the machine. A non ferromagnetic chain drives the system in translation, through a series of gears, by an outside motor. A digital display gives the position of the carriage. At one axial position there is a mechanism (see Fig. 2) for translating the "sigma" in the horizontal direction (perpendicular to machine axis (z)). After an x displacement is performed the carriage may again be scanned along the z direction.

IV TYPICAL APPLICATIONS

To illustrate the performance of the optical carriage we present here a selection of preliminary results. These results have been obtained in the LMP device with a barium Q-plasma with a density between 10^9cm^{-3} and 10^{10}cm^{-3} .

A Grotian diagram of BaII is shown in Fig. 3(a). The $5^2D_{5/2}$ and $5^2D_{3/2}$ are metastable states (life time $\sim 1\text{s}$) and they represent respectively 9% and 11% of the ion density produced by the plasma source. LIF was performed by exciting the $5^2D_{3/2} - 6^2P_{3/2}$ transition with a cw dye laser tuned at 585.4nm and observing the fluorescent light at 455.4nm. Laser excitation of transitions from the ground state were not possible with our cw dye laser system. Excitation of transitions from the ground state were performed using a pulsed dye laser.

A) OPTICALLY MEASURED WAVE INTERFEROGRAMS

Electrostatic waves are detectable through coherent oscillations in the ion

distribution function. These oscillations can be observed directly and nonperturbatively as a function of position and ion velocity along the laser beam using LIF. In the experiment, the electrostatic wave is launched using four rings ($\phi=4\text{cm}$, width=1cm) coaxial with the static magnetic field. The antenna ring spacing may be continuously adjusted from outside the vacuum chamber in order to match the parallel wavenumber k_{\parallel} with a minimum of wave damping. Oscillations in the ion distribution, which are coherent with the signal applied to the antennae, are detected by a lock in amplifier (Fig. 3(b)). Spatial phase progression of the wave is measured while the carriage is scanned along the machine axis (Fig. 3(c)). Using this technique it is possible to measure wave amplitudes below the level detectable with probes.⁷

B) SLOW ROTATION OF THE PLASMA COLUMN MEASURED BY THE OPTICAL TAGGING TECHNIQUE

It is well known that in a single ended Q-device, the plasma is drifting from the hot plate to the endplate; this velocity in our device is typically $\sim 1.1 \cdot 10^5 \text{ cm} \cdot \text{s}^{-1}$. Superposed on this drift, the plasma may have a slow rotation⁸. In many cases, this rotation is so slow that the corresponding Doppler shift is hidden by the thermal Doppler broadening of the line. The tagging technique permits measurement of extremely slow rotations of a plasma column and is not limited by Doppler broadening. Figure 4(a) shows the experimental set up. A tag beam crosses the edge of the plasma, and downstream a search laser beam is scanned across the plasma to look for tag particles. For this experiment the bright signal scheme has been utilized. A pulsed dye laser (10ns pulse length) tuned to 493.4nm increases the population of the metastable state $5^2D_{3/2}$ by exciting transitions between the ground state and the $6^2P_{1/2}$ level. A telescope looking at the tag position monitors the intensity of the 649.7nm transition, which is a measure of the density of tagged particles. A cw dye

laser (the search beam) tuned at 585.4nm measures the population of the $5^2D_{3/2}$ metastable state by inducing fluorescence at 455.4nm. The burst of tag particles detected on the 455.4nm line contains information about the parallel drift, thermal spreading and rotation of the plasma. From the time of flight of the tagged particles measurements of plasma drift and thermal spreading are obtained which agree with standard LIF measurements parallel to the magnetic field. Tagged particles have been followed over a distance of 73.5cm. This limit is due to a technical constraint on the tag beam access. If a boxcar is used for signal overaging, it is necessary to change the gate timing as the carriage scans to accommodate changes in the time of flight between the tag and search beam.

Having observed the presence of the tag particles in the search volume at two discrete axial positions, a lower bound on the rotation of $6.4 * 10^3$ rad/sec was obtained. (With each subsequent measurement, the possibility of additional rotations between the points of measurement can be eliminated.) A Doppler shift measurement confirmed that this lower bound was indeed the rotation velocity in addition to determining the sign. In principle, it is only necessary to measure the parallel drift speed and the axial separation of the helical "winding" of the tag particle orbits to measure the rotation speed. The direction must be determined from the sense of the helix.

The sensitivity limit of the method can be simply estimated by

$$\dot{\theta}_{\min} \text{ [rad sec}^{-1}\text{]} = \frac{\pi v_{\text{drift}}}{d} \sim 900 \text{ rad/sec}$$

In LMP device, $v_{\text{drift}} \cong 1.1 \cdot 10^5 \text{ cm} \cdot \text{sec}^{-1}$, d is in principle limited by the plasma length (~400cm). In our case θ_{\min} corresponds to particles which rotate half a turn

between the tag and search beam. the time of flight $(v_d/d)^{-1}$ in the LMP determines the limit of resolution, and is much shorter than either the lifetime of the metastable state (~ 1 sec), or the characteristic radial diffusion time of this quiescent plasma.

In summary, we have developed a nonperturbative optical probe for LIF in a magnetized plasma. This probe has greatly improved access to the plasma. Preliminary results obtained with the "optical carriage" are promising. Further experiments are in progress to investigate wave-particle interactions including the phenomena of intrinsic stochasticity ^{6,7}.

ACKNOWLEDGEMENT

The authors would like to thank P. Gorgerat, R. Lassueur and J.P. Bärtschi for their skillful and accurate technical assistance. Professor N. Rynn from the University of California at Irvine has kindly lent the cw dye laser equipment which was essential for the optical tagging experiment. We also express our appreciation to Dr. H. Van den Bergh of the EPFL and to Spectra Physics for lending laser components. This work was supported by grants from the Swiss Fonds National de la Recherche Scientifique and by the U.S. National Science Foundation.

REFERENCES

- ¹ R. Koslover and R. McWilliams, Rev. Sci. Instrum. 57, 2441(1986)
- ² F. Anderegg et al., Phys. Rev. Lett. 57, 329 (1986)
- ³ R.A. Stern, D.N. Hill and N. Rynn, Physics Lett. 93A, 127 (1983)
- ⁴ P. Kohler et al. in Proceedings of the International Conference on Plasma Physics, Lausanne, Switzerland, 27 June - 3 July 1984 edited by M.Q. Tran and M.L. Sawley (CRPP, EPFL, Switzerland 1984) Vol. 2, p.317
- ⁵ P.J. Paris, Internal Report CRPP INT137/87
- ⁶ F. Skiff, F. Anderegg and M.Q. Tran, Phys. Rev. Lett. 58, 1430 (1987)
- ⁷ F. Skiff and F. Anderegg, Phys. Rev. Lett. 59, 896 (1987)
- ⁸ H.W. Hendel and P.A. Politzer, Princeton Plasma Physics Laboratory Report No. MATT-507 (1967)

FIGURE CAPTIONS

Fig. 1(a) - Principle of LIF

Fig. 1(b) - Principle of optical tagging(bright signal)

Fig. 2 - Schematic view of the optical probe : 1) Injection of light in the plasma : fiber, lens and polariser; 2) Beam dump; 3) Concave reflecting mirror; 4) Collecting optics; 5) Fiber bundel; 6) Vacuum passage to the PMT outside vacuum chamber; 7) Mechanism for translating the "sigma" in the horizontal direction (perpendicular to machine axis (z)); 8) Three rod allowing translation of the "sigma" along the machine axis; 9) Vacuum vessel.

Fig. 3(a) - Goterian diagram for Ball.

Fig. 3(b) - Experimental set-up for optical wave interferogram.

Fig. 3(c) - Optically measured wave interferogram 30kHz $\lambda_{||} \cong 5.5\text{cm}$.

Fig. 4(a) - Experimental set-up for optical tagging.

Fig. 4(b) - Radial profile seen with the search laser 63.5cm downstream from the tag beam. Dashed curve is the radial density profile.

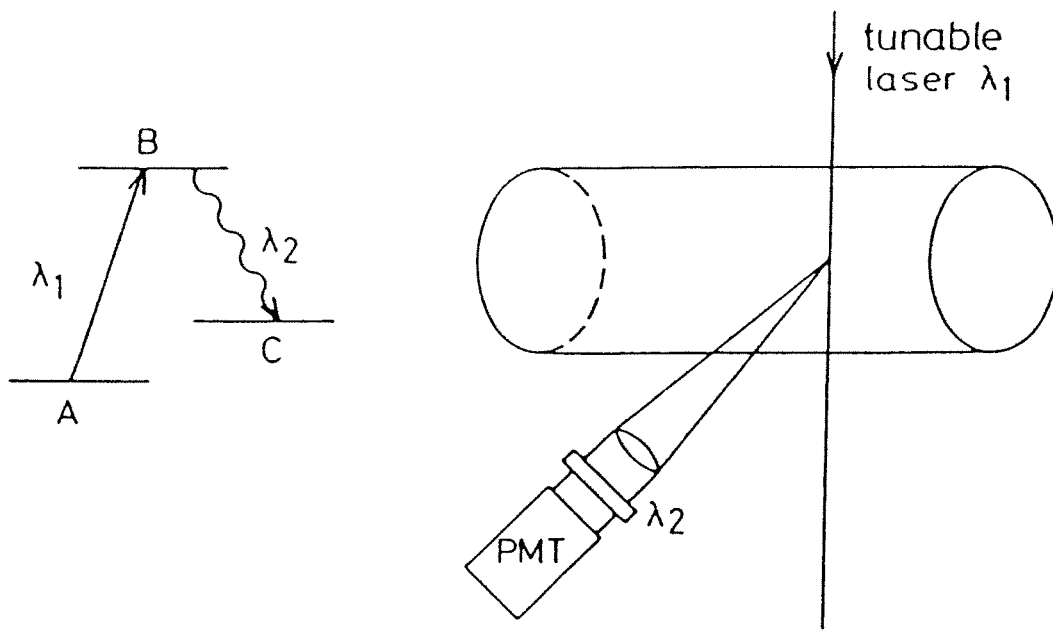


Fig. 1a

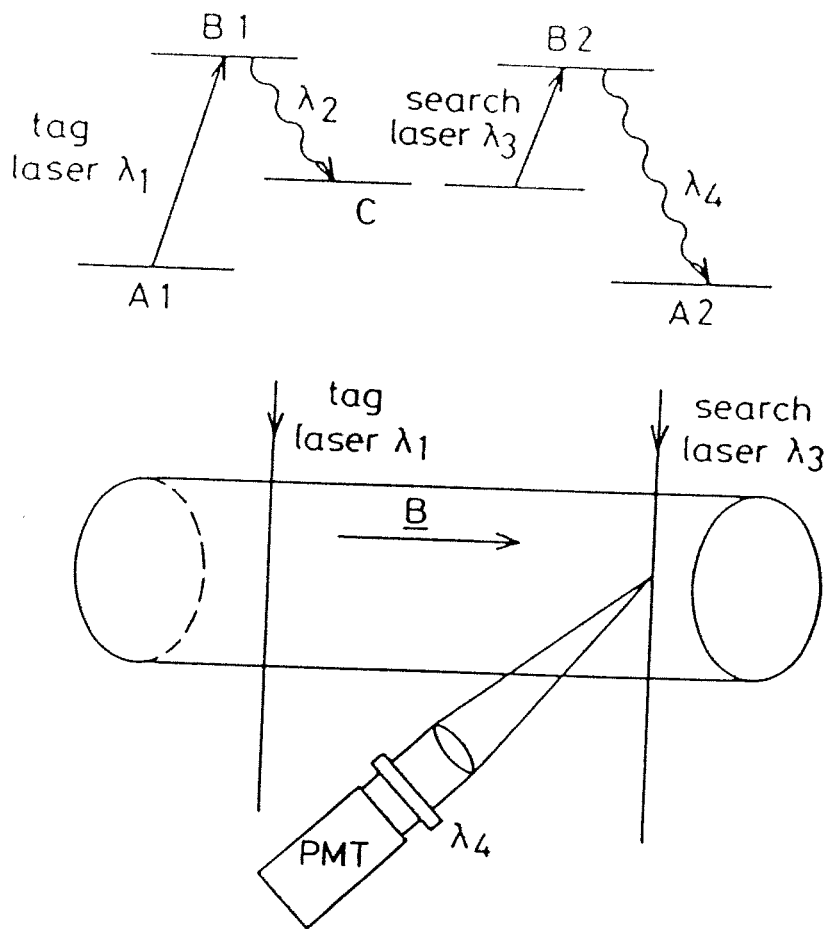


Fig. 1b

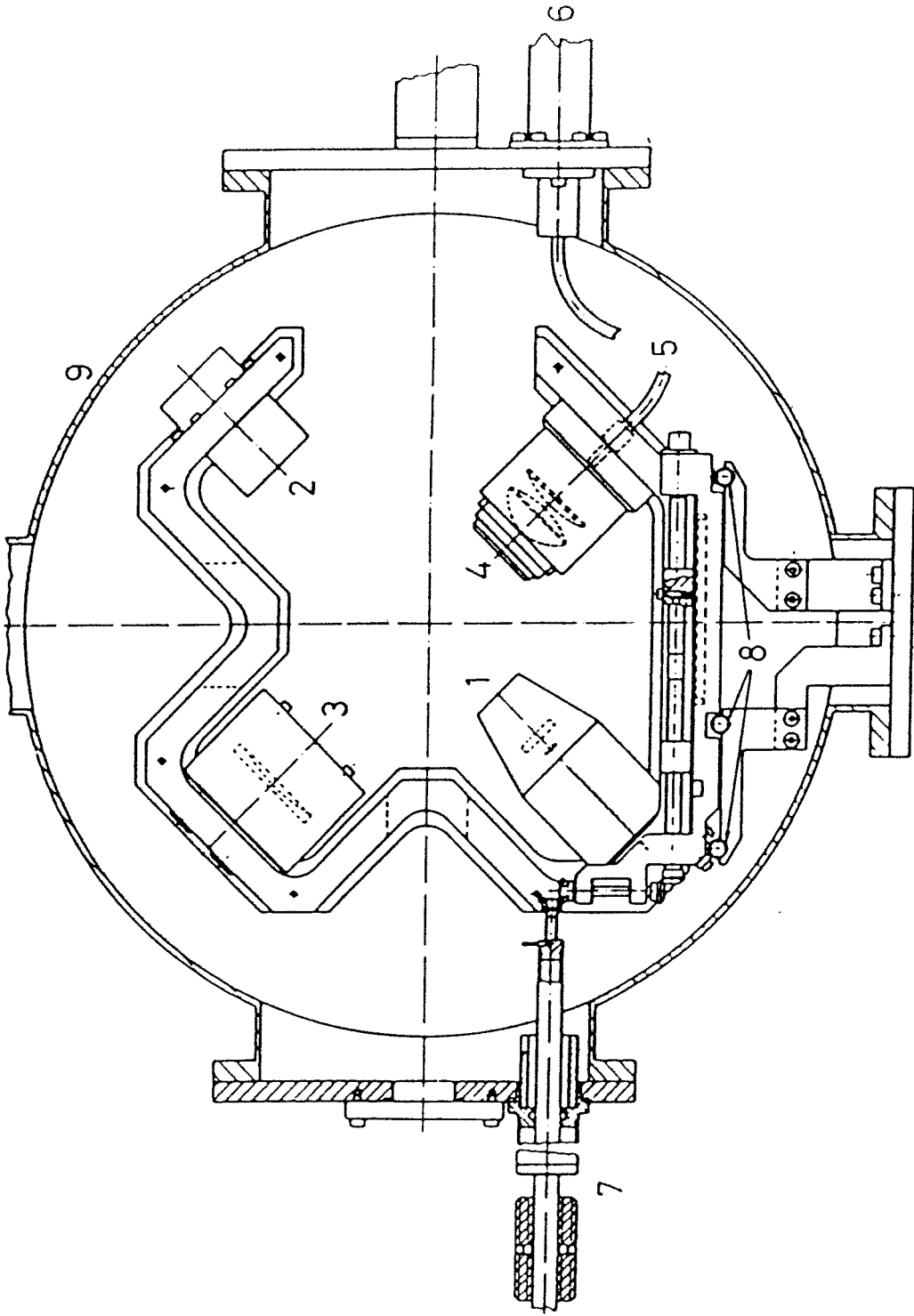


Fig. 2

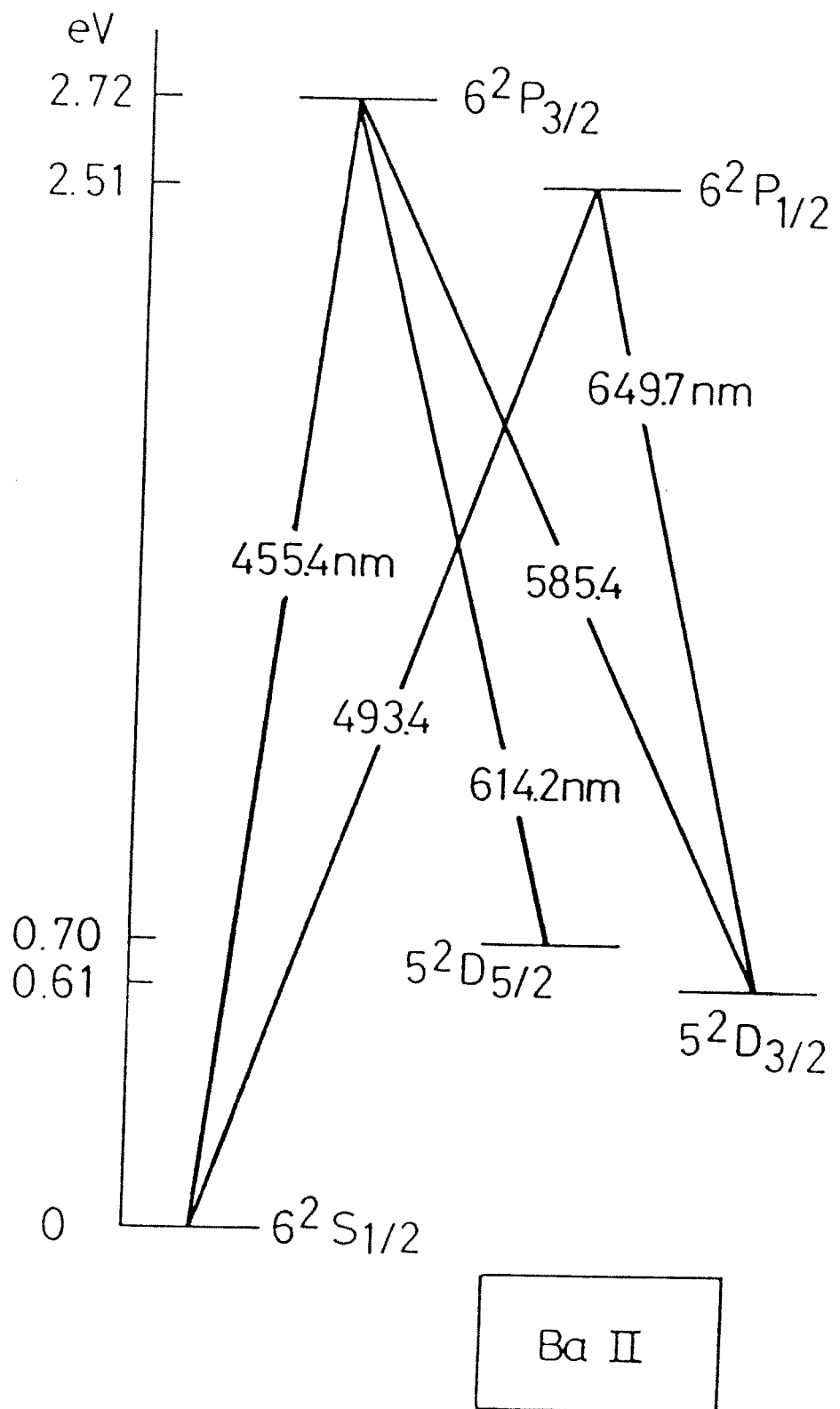


Fig. 3a

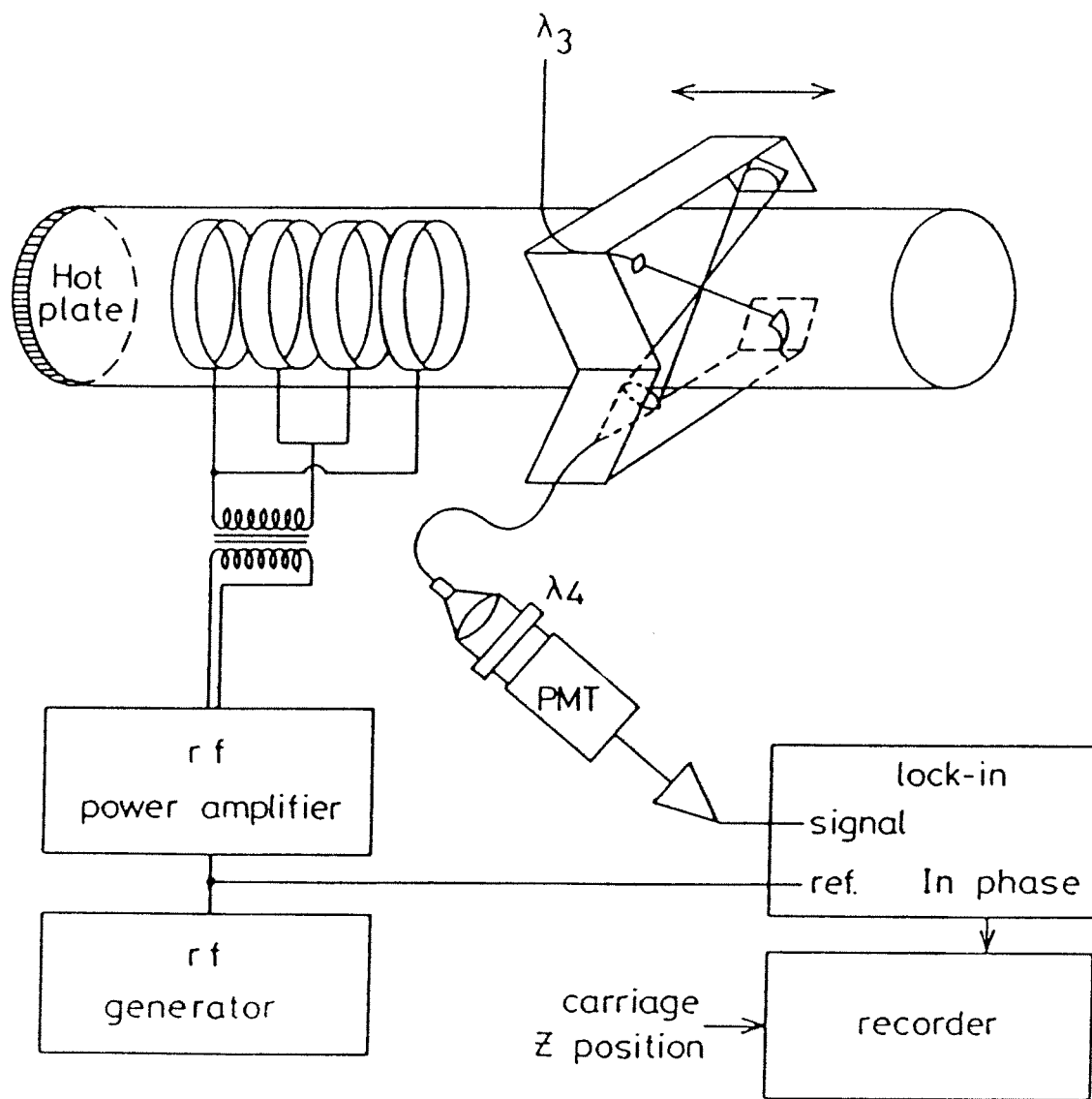


Fig. 3b

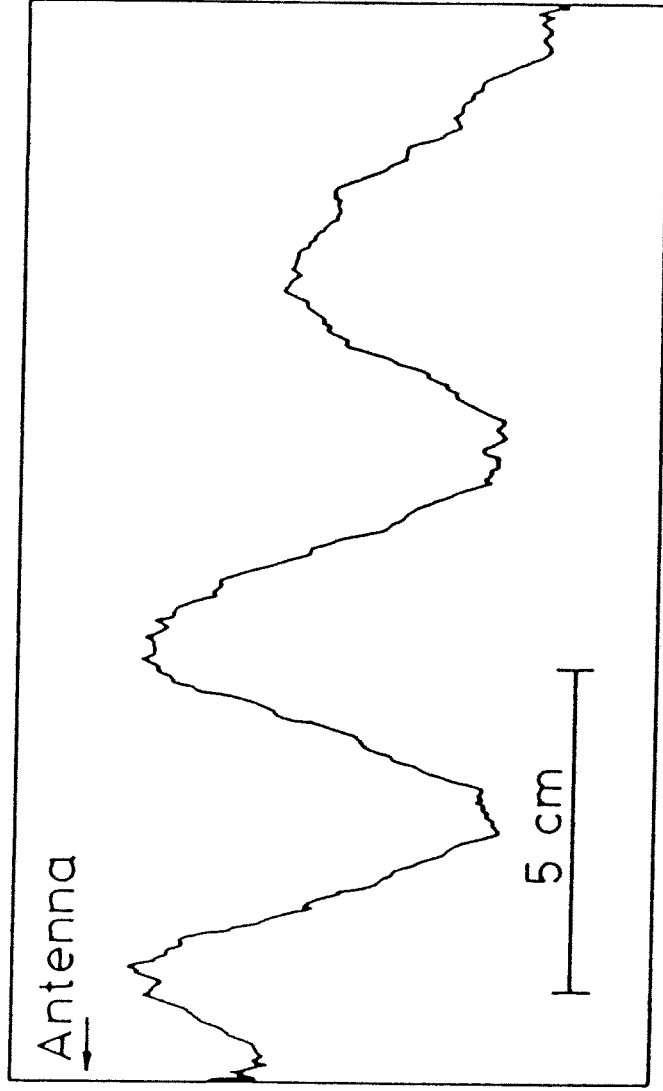


Fig. 3c

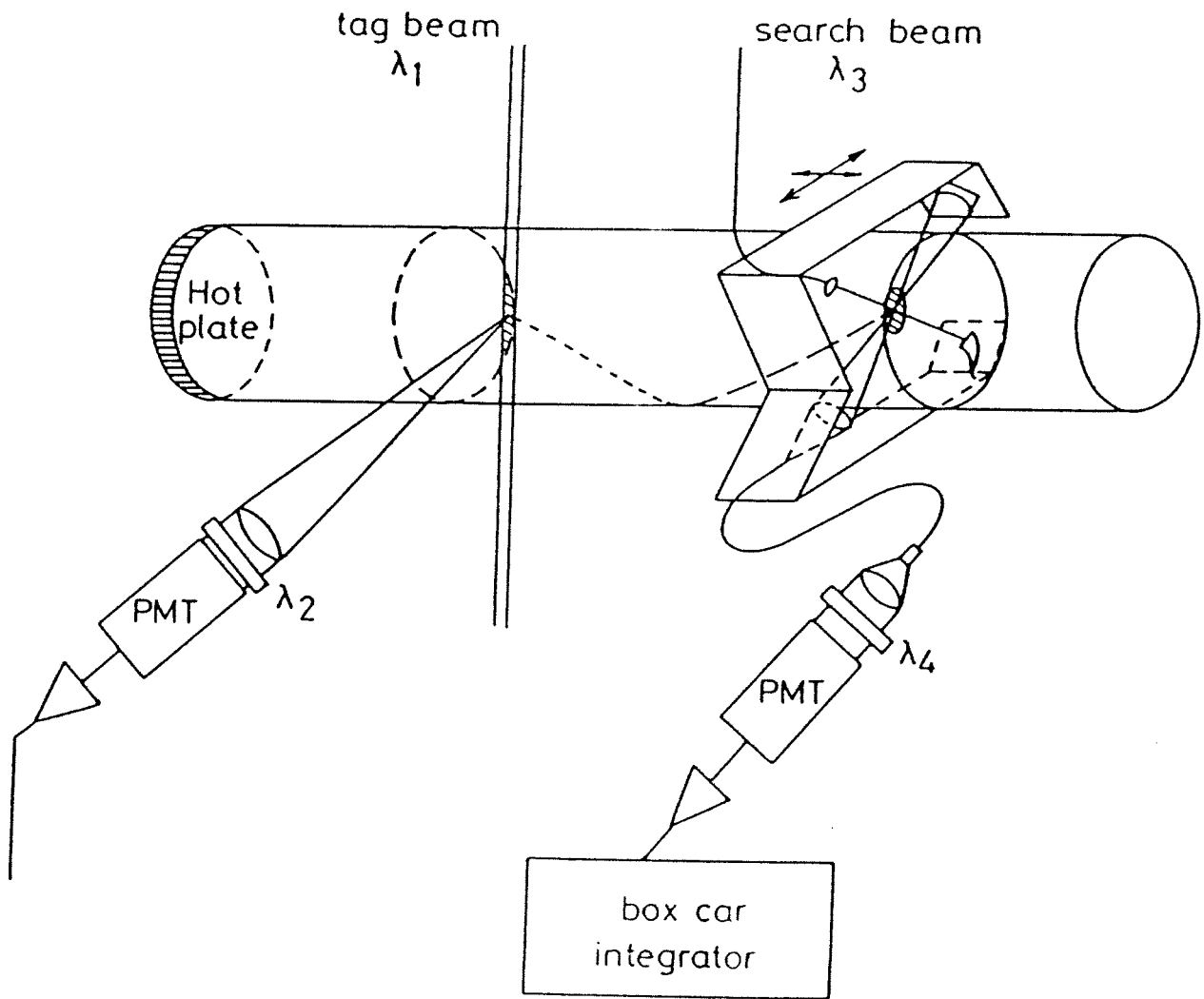


Fig. 4a

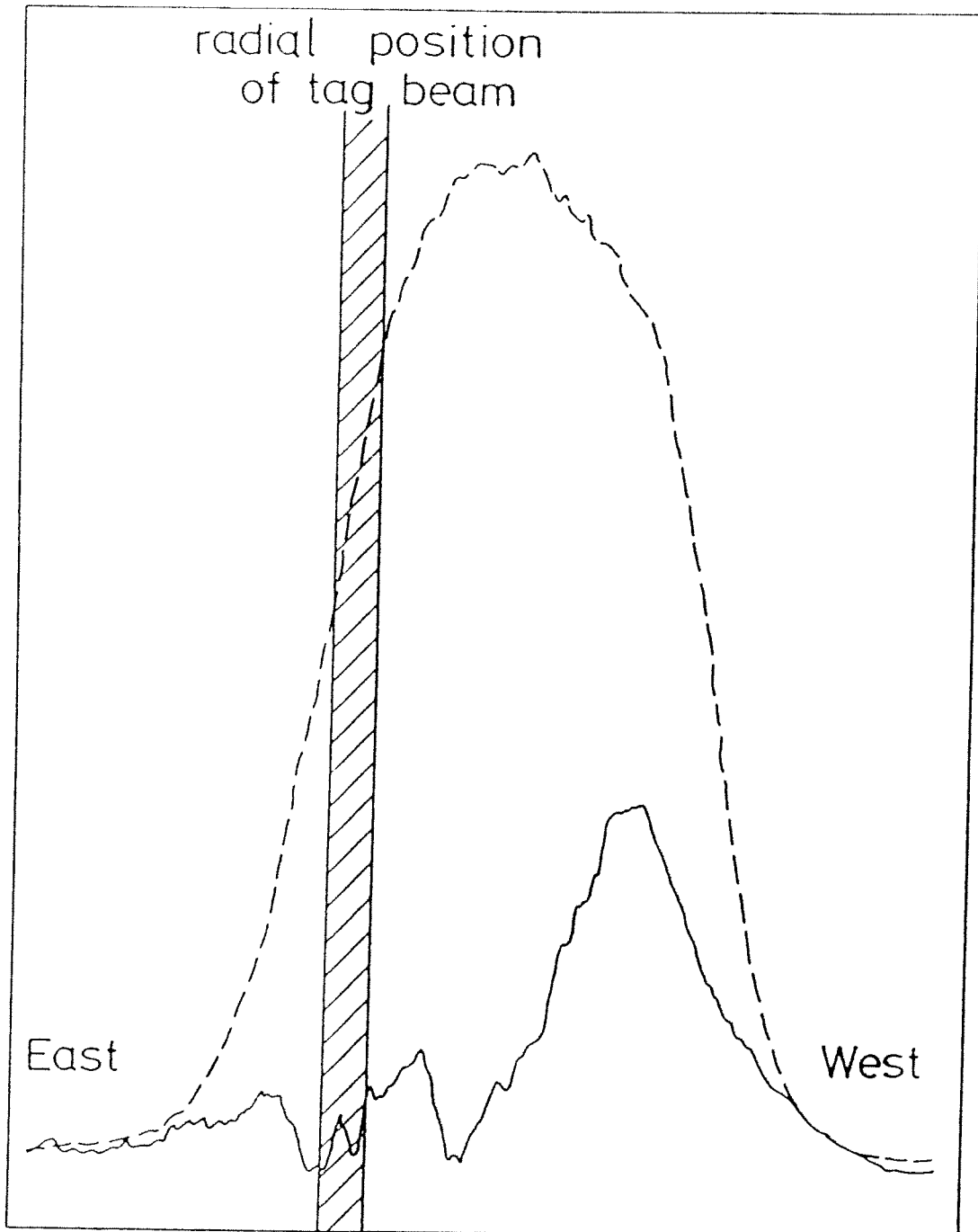


Fig. 4b

